

Analysis of Soil Contamination Effects on Maize Plant using UAV-Mounted Multispectral Camera

Massimiliano Gargiulo^{1†}, Claudia Savarese¹, Francesco Tufano¹, Sara Parrilli¹, Cesario Vincenzo Angelino¹,
Mariavittoria Verrillo^{2,3}, Vincenza Cozzolino^{2,3}, Alessandro Piccolo^{2,3}, and Marco De Mizio¹

¹Italian Aerospace Research Centre
Via Maiorise snc, 81043 Capua, Italy
m.gargiulo@cira.it

² Dipartimento di Agraria, Università di Napoli Federico II
Via Università 100, 80055 Portici, Italy

³ Centro Interdipartimentale di Ricerca per la Risonanza Magnetica Nucleare per l'Ambiente,
l'Agroalimentare, ed i Nuovi Materiali, CERMANU
Università di Napoli Federico II, Via Università 100, 80055 Portici, Italy

[†]Corresponding author

Abstract

Toxic substance contamination of the environment is a major issue. Remote sensing, which employs unmanned aerial vehicles (UAVs) equipped with multispectral or hyperspectral sensors, provides high-resolution data without requiring destructive samples and can detect plant distress before visual symptoms occur. In this study, the effect of potentially toxic elements (PTEs) and polycyclic aromatic hydrocarbons (PAH) soil contamination on maize plant development was examined using multispectral data from a UAV, and preliminary results with the usage of hyperspectral are discussed. The findings of this work demonstrate the utility of UAV-based multispectral and/or hyperspectral analysis in predicting characteristic plant changes caused by soil changes, giving useful information for improving environmental monitoring efficiency.

1. Introduction

The problem of soil pollution is a widespread phenomenon worldwide and has severe impacts on human health and the ecosystem.¹ In particular, heavy metals are among the most dangerous pollutants as they do not degrade naturally and can accumulate in the soil, contaminating both the soil and groundwater. The combined use of plant knowledge and earth observation techniques constitutes an innovative element to improve environmental monitoring capabilities. The key element is the ability of vegetation to function as a "sentinel" for multiple phenomena. In fact, several plants are able to function as bio-indicators, modifying their characteristics when exposed to certain pollutants. The chemical/physical changes that these bio-indicators show when subjected to stress often result in alterations of their optical properties and can therefore be "read" by different remote sensors. The activities described in this work are part of the STOPP ("Earth Observation Tools and Techniques in Proximity and Persistence") project, funded by the Italian Space Agency (ASI). One of the objectives of the project is to investigate the relations between pollutants and bioindicators and the potential applications of an environmental monitoring system based on the acquisition of data from sensors installed on proximal and remote sensing platforms. The usage of small unmanned aerial vehicles (UAVs) equipped with multispectral, hyperspectral or thermal sensors is becoming increasingly relevant in environmental monitoring.² In particular, the use of multispectral data collected from a UAV allows for the detection of changes in the plants' spectral characteristics, providing valuable information on a wide variety of uses, including plant distress detection, soil moisture assessment, and crop monitoring. Furthermore, information on the impact of soil contamination on plant development thanks to high-resolution data of the proximal and remote sensing sensors can be obtained without further requiring destructive samples.³⁻⁶

Maize is a staple crop and an essential source of food for many people worldwide. In particular, it is the second forage species cultivated in the Campania Region, also including the area referred to as "The Triangle of Death", the area on which the studies of the STOPP project focus.⁷ UAV technologies have often been exploited to determine the impact of environmental conditions on crop yield, especially to predict production losses or to manage the irrigation system with minimal disturbance to the plants.^{8,9}

SHORT PAPER TITLE

UAV-based multispectral data has a wide range of environmental monitoring applications, including soil pollution studies and maize plant monitoring.^{5,10} The findings of some studies show the efficacy of UAV-based data in forecasting distinctive plant changes caused by soil changes, emphasizing the need of utilizing this technology to improve the effectiveness of environmental monitoring operations.

This study focuses on the use of multispectral and hyperspectral data acquired in proximal sensing using mini-UAV systems to examine the effect of soil contamination caused by potentially toxic elements (PTEs) and polycyclic aromatic hydrocarbons (PAH) on maize plant development. The findings of this study highlight the importance of this technology in maize fields monitoring and the potential utility of these data within a bioindicator-based environmental monitoring paradigm. This work is organized as follows. The experimental setup is described in Section 2. After that, Section 3 describes the proposed methodology. The findings are then examined, followed by an analysis of the results in Section 4 and potential future work in the last sections.

2. Experimental Setup

2.1 Soil contamination and humic treatment

The soil used in the experimentation was collected from the surface layer (0 - 20 cm) of clayey agricultural soil at the experimental farm of the University of Naples Federico II, located in Castel Volturno (CE). The soil was developed on ash and pumice pyroclastic parent material, and characterized by the following general properties: Vitrandic Haplucept (USDA soil taxonomy), 8.5 pH (H_2O), 24 % sand, 36 % silt, 40 % clay, 1.05 % organic carbon, 0.17 total nitrogen, 28.2 $cmolkg^{-1}$ cation exchange capacity, 98.7 gkg^{-1} total carbonates. After sampling, the soil was air-dried, sieved (5.00 \emptyset sieve) and stored at room temperature for the contamination process. The concentrations used in the experimentation were chosen on the basis of the soil contamination thresholds described by the Italian legislation (D.Lgs. 152/2006), as exceeding tolerable levels of soil quality. In detail, the soil was spiked by adding 300 ml of an aqueous solution containing a mixture of three inorganic contaminants (Zn, Pb, Cr) and benzopyrene to each pot (2.5 kg), considering soil field capacity. After spiking, soil samples were incubated at room temperature for 10 days while moisture was maintained at field capacity. The final concentration of each pollutant is reported in Table 3. The humic substances used in the experimentation were extracted from a green compost produced in the composting facility of the same experimental farm of the University of Napoli Federico II at Castel Volturno (CE). Compost was obtained by the composting process of a static pile consisting of both horticultural and coffee residues under forced air insufflation. Humic Substances (HS) were obtained by a KOH alkaline extraction from the dried compost and used in the form of dried powder for the humic acid treatments. Briefly, humic solutions of 10 gL^{-1} were prepared by dissolving the humic acid powder extracted from the green compost in distilled water. The humic solutions were then added to each soil sample by supplying 50 mL per pot at two different times of plant development: (i) at the transplant and (ii) at three weeks after sowing.

Table 1: Experimental Setup.

Name	Treatment	# Replicates
A	Control (Untreated)	12
B	Spiked Soil	12
C	Control + HS	4
D	Spiked + HS	4

2.2 Plant Experiment

Maize seeds (*Zea Mays* L.) were sown in the soil pots and grown from September to December 2022, under greenhouse conditions at ambient temperature (15-25 °C) and natural light. Basal fertilization (120, 60, and 166 $mgkg^{-1}$ of N, P and K, respectively) was applied to all soil pots, while the water-holding capacity of the soil was maintained between 40 and 70 % throughout the experiment. The experimental design consisted of the following thesis, as reported in Table 1: control (untreated, A), spiked soil (B), control plus humic acid treatment (C), and sparked soil plus humic acid treatment (D). The control A and spiked thesis B were replicated 12 times, while the humic acid treatments (C and D) were both replicated four times. Sampling was performed eleven weeks after sowing, collecting the youngest and fully expanded leaves. Biomass was determined (fresh and dry weight) to provide the plants yield for each treatment.

2.3 Micasense Altum

The Micasense Altum is a compact and high-performance multi-spectral and thermal imager for UAV mapping.¹¹ It collects imagery in 5 spectral bands (blue, green, red, red edge, near-infrared as shown in Tab.2) and thermal. It has a 48-degree-by-37-degree field of vision with a GSD of 5.2 cm at 120 meters, making it excellent for plant phenotyping. In addition to its image sensor specs, the Micasense Altum is equipped with a GPS and a Downwelling Light Sensor

Table 2: The Micasense Altum bands

Name	Center	Bandwidth
Blue	475 nm	20 nm
Green	560 nm	20 nm
Red	668 nm	10 nm
Red edge	717 nm	10 nm
Near infrared	840 nm	40 nm

(DLS). The DLS is an advanced incident light sensor that connects directly to the camera. During a mission, the DLS measures the ambient light and sun angle and records this information, along with GPS location, in the metadata of the captured images by the camera. This information can then be corrected for global lighting changes in the middle of a flight, such as those that can happen due to clouds covering the sun. Jointly using the recorded metadata and an appropriate calibration panel, it will be possible to compare acquisitions made at different times.

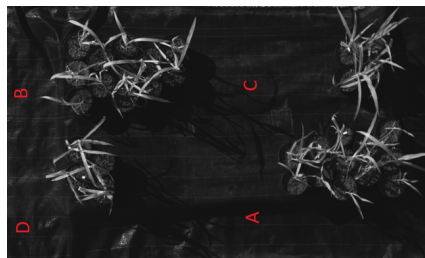


Figure 1: Configuration of plants arrangement.

3. Proposed Analysis

3.1 Test Description

To carry out the experiment, a customized Foxtech Hover 1 quadcopter has been used.^{12,13} The drone was equipped with the Micasense Altum camera and its DLS, as shown in Fig. 4. In order to ensure the right light acquisition, the DLS was installed on top of the drone. The camera is, however, installed on the bottom of the vehicle without the gimbal. In this way the camera and its Downwelling Light Sensor are integral. The drone's original battery has been replaced with a more performing one, capable of higher current despite the autonomy. In this configuration, the complete system weight is around 3.5 kg with battery autonomy of approximately 20 minutes. The Drone performed

Table 3: The used doses of soil pollutants.

Pollutants	Limit concentration $mgkg^{-1}$	Reagents Reagents	Used dose $mgkg^{-1}$
Cr	150	$CrCl_3 \cdot 6H_2O$	450
Pb	100	$PbCl_2$	300
Zn	150	$ZnSO_4 \cdot 7H_2O$	450
Benzopyrene	0.1	benzopyrene	0.3

SHORT PAPER TITLE

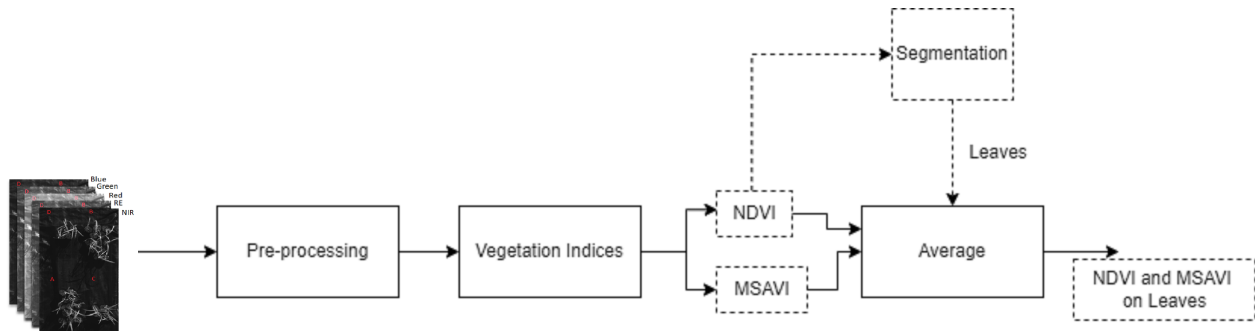


Figure 2: Workflow on Micasense Altum bands.

two flights on plants grown in pots by Cermanu at the Reggia di Portici On November 8, 2022, and December 7, 2022. The camera frame rate and drone flight plan were set, respectively, to 1 FPS and at an altitude of 15 m. In this way, we obtained a GSD approximately equal to 0.4 mm and it was possible to avoid the waving tree phenomena induced by the airstream generated by drone propellers. Regarding these drone flights, we segregated the area and ensured that all individuals present were under mission control. In the next experiments, we will be flying at higher altitudes in accordance with regulations. Before take-off, a camera calibration phase is needed. Figure 3 shows the calibration panel used.



Figure 3: Calibrated Reflectance Panel.

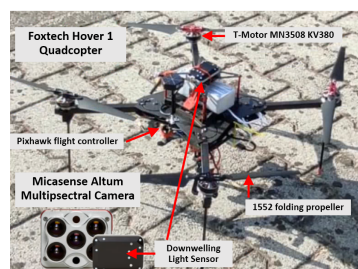


Figure 4: The customized Foxtech Hover 1 quadcopter.

The contaminated (B-D) and non-contaminated (A-C) plants were arranged following the configuration shown in Fig. 1 (the NIR image is shown in one of the acquired frames). Treatments C and D have a treatment with humic substances. The acquired dataset contains both images with all the samples of the experiment and images with only a subset of them. Using images with partial plant coverage, in this phase of the project, is useful to investigate the techniques to generate orthophoto and 3d reconstruction. This arrangement aimed to simulate as much as possible a canopy analysis, which is not currently possible, so it was decided to carry out an analysis only on the pixels related to the leaves.¹⁴

3.2 Proposed Image Processing

Due to the close proximity of the drone to the object or to the significant variation in distances between the captured objects in the images, the acquired data comprising 5 bands exhibits a pronounced spatial misalignment. This misalign-

ment was compensated by exploiting the subpixel image registration by cross-correlation, proposed by.¹⁵ This registration provides the same degree of accuracy as the FFT upsampled cross-correlation method while requiring substantially less calculation time and memory. The used registration begins by utilizing an FFT to acquire an initial estimate of the cross-correlation peak. It then increases the accuracy of the shift estimation by using a matrix-multiply DFT to upsample the DFT in close proximity to that estimate. This approach ensures that the upsampled cross-correlation is computed using all picture points.

In Fig. 5, the RGB false-color image with the misalignment and the corrected one are shown. The drone serves as a flying camera carrier, with all picture processing handled by specialist software. After the preprocessing phase, we consider the Normalized Difference Vegetation Index (NDVI) and Modified Soil-Adjusted Vegetation Index (MSAVI) between the plethora of vegetation indices commonly used by the remote sensing community.¹⁶⁻¹⁸ The considered indexes are both commonly used in remote sensing and they take advantage of different reflection modes of vegetation at red and NIR wavelengths.

Thus, starting from the preprocessed image, the NDVI and MSAVI were calculated using the following definitions:

$$NDVI = \frac{NIR - RED}{NIR + RED}$$

$$MSAVI = \frac{1}{2} \left((2 \cdot NIR + 1) - \sqrt{(2 \cdot NIR + 1)^2 - 8 \cdot (NIR - RED)} \right) \quad (1)$$

where NIR is the Near-infrared band, centered at the wavelength of 840 nm (for multispectral camera), and the band closer to the central wavelength of 770 nm for the hyperspectral camera; while RED is the Red band, centered at 668 nm (for the MS camera), and the band closer to the central wavelength of 650 nm for the hyperspectral. On one hand, the

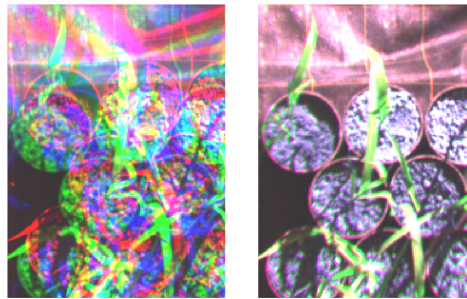


Figure 5: In the image on the left there is a visible misalignment in RGB that was compensated in the image on the right.

NDVI is a simple and easy index to calculate that it is widely used to assess the health and/or productivity of vegetation. On the other hand, the MSAVI is designed to correct for the effect of the soil on the values of NDVI.¹⁹ In particular, by exploiting the NDVI, an unsupervised segmentation was carried out in order to isolate only the leaves within the image, in order to simulate a "canopy", i.e. a field in which all the pixels were covered by maize plants. Thus, we used a segmentation based on a threshold, obtained as the mean between the centroids obtained from the two-class k-means on the NDVI index. This threshold is applied to the NDVI index to have a two-class vegetation (leaves)/non-vegetation segmentation. At this point, we have reported on the leaf pixels average values of NDVI and MSAVI for each of the described treatments.²⁰ After restricting our analysis to the leaves, we use a morphological opening operation to eliminate the thin spots on the obtained image segmentation. In Fig. 2, the phases of the described processing are summarized and replicated for acquisitions for both flights.

4. Results

Firstly, after the preprocessing phase on the images, we compare the different considered treatments based on the spectral signatures (with only 5 points, one for each band acquired). In Fig. 6, we showed the 4 different spectral signatures, but this analysis is not particularly informative. However, the greatest difference between the NIR and Red bands, which are used by the traditional vegetation indices, may be seen in the D treatment.

Another comparison was realized between the average values of NDVI and MSAVI on leaves' pixels for each treatment, derived from both acquisition dates (November 8, 2022, and December 7, 2022), which are reported in Tables 4 and 5. For each soil condition, the average values of the NDVI and MSAVI calculated on the leaves for the flight

SHORT PAPER TITLE

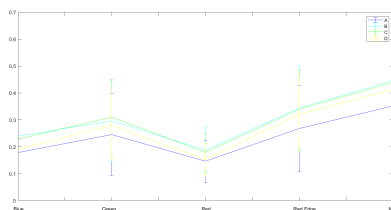


Figure 6: The spectral signatures of the four different contamination treatments.

on December 7, 2022, were also directly compared with the dry biomass, as shown in Figures 7 and 8. In particular, we found that plants grown in contaminated soils had higher values than the corresponding controls ($B > A$ e $D > C$), in line with the results of the biomass analysis.²¹ In fact, the addition of PTE and PAH pollutants in the soil only slightly affected maize growth, as it was revealed by similar shoot dry matter weights measured at harvest for treatments A-B and C-D. These results are in contrast with the widely reported toxic effect on corn development of both heavy metals and PAH.²² A possible explanation concerns the physical-chemical properties of the soil used for the experimentation, which is characterized by high carbonates content, alkaline pH and low organic carbon amount. These soil characteristics may have adversely affected maize plants development even in the uncontaminated control treatments (Figures 7 and 8). Indeed, it has recently been reported that calcareous soils possess poor physicochemical characteristics, such as low soil-water relations, soil crusting, and insufficient nutrients availability, which could cause chlorosis and stunted plants growth.²³ These adverse soil conditions can also alter several plants physiological processes, including leaf morphology, chlorophyll synthesis, and photosynthetic efficiency, which probably induced a change in the spectral response of the control maize plants. On the other hand, the similar or even slightly higher biomass production observed for corn plants grown under spiked soils (B-D) as compared to their controls (A-C) (Figures 7 and 8) could be related to the poor mobility and bioavailability of the applied pollutants. For example, an elevated pH and the presence of carbonates in the soil leads to an increased retention of heavy metals, mainly lead (Pb) and chromium (Cr), as reported in.²⁴ Furthermore, the addition of zinc (Zn) may have positively affected maize plants growth, since this crop is highly sensitive to Zn deficiency, whose bioavailability is reduced by some soil proprieties such as the high pH and carbonates content, and the low quantity/quality of organic matter.²⁵ In plants, zinc plays a key role in many important biochemical pathways, such as photosynthesis and the integrity maintenance of biological membranes,²⁶ that indirectly influence the leaf spectral response. Therefore, the external amount of Zn supplied in B and D treatments may have facilitated the development of maize seedlings in the alkaline-calcareous soil used for the experimentation. In fact, as already described, we found slightly higher values of vegetation indices for these plants.

4.1 Physical, chemical and biological properties

The comparison between the NDVI and MSAVI indices calculated on the leaves for the flight on December 7, 2022 also revealed higher values for plants grown in soils added with humic substances than untreated ones, which means $C > A$ and $D > B$. Again, this result is consistent with that of the biomass analysis. In fact, the addition of humic substances (HS) in both uncontaminated (C) and spiked soil (D) significantly improved the shoot biomass of maize plants (Figures 7 and 8). These results are in line with the widely demonstrated role of HS in improving soil physical, chemical and biological proprieties. Humic substances (HS) are relatively small heterogeneous molecules resulting from the biotic transformation of plant and animal tissues and held together by multiple weak interactions in supramolecular associations.²⁷ It has been shown that the addition of humic matter leads to better soil quality by enhancing aggregates stability, regulating water flow, reducing run-off and erosion, influencing nutrient availability, and stimulating microbial proliferation.²⁸ Recently, humic substances were also found to be good complexing factors for many metal ions, since their several functional units (carboxylic, hydroxylic, phenolic, and aliphatic groups) influence the mobility and availability of contaminants in soil.²⁹ Furthermore, humic substances are recognized as plant biostimulants, as they can positively affect several plants physiological and metabolic processes as hormone-like molecules.³⁰ In particular, different crops treated with humic substances showed an increase in shoot and roots growth, chlorophyll content, photosynthetic efficiency and biosynthesis of essential compounds also involved in plant-stress tolerance.³¹ These studies all support the greater biomass production observed for maize plants under C and D soil conditions as compared with both A and B treatments, as well as the higher values of the calculated vegetation indices, which may indicate a better health status of these corn plants.

By repeating the same processing on images from the second flight, acquired on a different day, different average values are found, but some characteristics are maintained (in Table 5). The treatments with humic substances (C and

D) have higher average NDVI and MSAVI values compared to that without contamination. A clear distinction is found between treatments C-D and treatments A-B in terms of both average NDVI values and MSAVI values. In particular, between A and all other treatments the distinction in terms of NDVI average values is particularly distinguishable.

Basically, in both the acquisition campaigns, the first in November and the second in December, we have found that the NDVI and MSAVI values follow this trend: $D > C > B > A$.

Table 4: The mean values and standard deviations of NDVI and MSAVI for each soil contamination (SC) after 7 weeks from the sowing.

SC	NDVI	σ_{NDVI}	MSAVI	σ_{MSAVI}
A	0.3765	0.12	0.8616	0.18
B	0.3837	0.11	0.8980	0.17
C	0.4000	0.11	0.9028	0.18
D	0.4092	0.13	0.9090	0.19

Table 5: The mean values and standard deviations of NDVI and MSAVI for each soil contamination (SC) after 11 weeks from the sowing.

SC	NDVI	σ_{NDVI}	MSAVI	σ_{MSAVI}
A	0.3634	0.11	0.8773	0.16
B	0.4087	0.13	0.9110	0.18
C	0.4111	0.12	0.9437	0.17
D	0.4226	0.14	0.9582	0.18

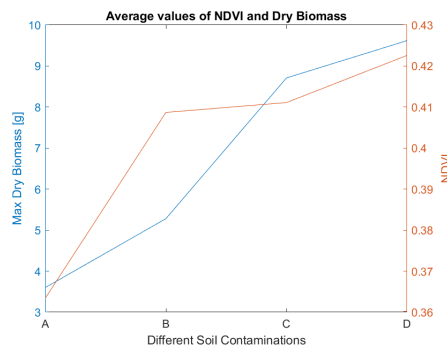


Figure 7: Comparison of the average values of the NDVI and the dry biomass.

A further analysis was made on the spatial resolution, noting that getting closer to the resolutions that could be obtained at higher altitudes, for example from a satellite or stratospheric platform, it is no longer possible to carry out a segmentation at the leaf level and therefore it is seen as the absence of a canopy leads to the impossibility of analyzing only the vegetation, given that inside the pixel the values also relating to the ground would fall. In fact, the NDVI values correspond to one vegetation absent in particular in this phase of growth, while the MSAVI values at one scarce vegetation, as shown in Table 6.

In conclusion, an analysis is needed in a phase in which there is a canopy, limiting the contribution of the soil, in particular, taking into account the resolutions towards which the project tends. Further, problems with image distortion, bad weather, and safety issues can arise for drone-based images. Utilizing image stabilization techniques, scheduling flights for the best weather, putting safety procedures into place, and adding redundancy measures are some ways to mitigate these difficulties.

4.2 Discussion and Future Perspective

The results obtained with the multispectral camera are, on average, in agreement with the data acquired through destructive biomass measurements. However, hyperspectral data can also be exploited for more specific analyses that

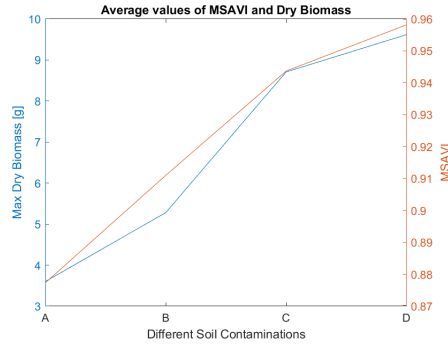


Figure 8: Comparison of the average values of the MSAVI and the dry biomass.

Table 6: $NDVI_{seg}$ and $MSAVI_{seg}$ represent the average values after the unsupervised segmentation step, instead $NDVI_{imm}$ and $MSAVI_{imm}$ represents the average values after an upsampling process.

SC	$NDVI_{seg}$	$NDVI_{imm}$	$MSAVI_{seg}$	$MSAVI_{imm}$
	0.3 - 0.4 mm	30 - 40 cm	0.3 - 0.4 mm	30 - 40 cm
A	0.3634	-0.0614	0.8773	0.4275
B	0.4087	-0.0529	0.9110	0.4300
C	0.4111	-0.0337	0.9437	0.4627
D	0.4226	0.0278	0.9582	0.5405

investigate the electromagnetic spectrum in greater detail. In our example, we considered a hyperspectral camera, the Cubert Ultris 5, which provides 51 bands covering the electromagnetic spectrum from 450 to 850 nm with a sampling interval of 8 nm. Such data allows for the preliminary results on the NDVI and MSAVI indices (Figure 7) to obtain the ability to distinguish between treatment with and without humic substances as for the Micasense Altum camera. Instead, further investigation on the capability of distinguishing the considered four treatments is needed. Currently, the shown analyses are only introduced to highlight the potentiality of the usage of hyperspectral data for future experiments. In particular, by observing the spectral signatures in Figure 9 distinguishing between pots with humic substances (HS) and pots without HS, we will possibly define an index with greater specificity for the given problem.

Table 7: $NDVI_{seg}$ and $MSAVI_{seg}$ represent the average values after the unsupervised segmentation step.

SC	$MSAVI_{seg}$	$NDVI_{seg}$
A + B	0.8632	0.8164
C + D	0.8743	0.8234

5. Conclusion

This study demonstrates the feasibility of using drone-based multispectral and hyperspectral analysis to assess the impact of different treatments on plant growth. The results indicate that drone-acquired data can effectively detect subtle changes in maize plant growth when exposed to a mixture of heavy metals and polycyclic aromatic hydrocarbons. In particular, the results obtained with the multispectral UAV pave the way forward, and hyperspectral data enables further exploration of spectral signature analyses to extract more specific indications, leveraging its superior spectral resolution. Although the findings from the multispectral imaging system highlight a promising trajectory and the utilization of hyperspectral data offers deeper insights into spectral signatures, leading to more specific and targeted conclusions, further research is necessary to fully validate these results. This study provides valuable insights and lays the foundation for future studies. Additionally, it highlights the significance of remote sensing technology, such as mini UAVs, for monitoring soil contamination and vegetation health.

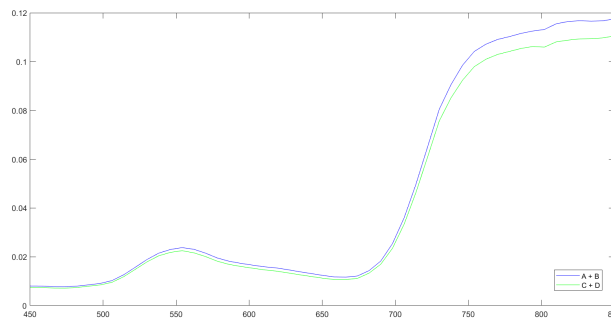


Figure 9: The spectral signatures from the hyperspectral camera (Cubert Ultris 5) for the treatments with and without the humic substances (HS).

ACKNOWLEDGMENT

The authors would like to express their gratitude to the Italian Space Agency (ASI), which funded the project, and the other partners for their assistance and contributions to this effort. The funding supplied has made a significant impact on the quality and advancement of our results.

The paper should not exceed 15 pages. Please upload your file in plain portable document format (pdf) only, i.e. the file should not be protected nor in any other format. The submitted pdf file should not exceed 5 Megabytes.

References

- [1] C. Govindasamy, M. Arulpriya, P. Ruban, L. F. Jenifer, and A. Ilayaraja, "Concentration of heavy metals in seagrasses tissue of the palk strait, bay of bengal," *International journal of environmental sciences*, vol. 2, no. 1, pp. 145–153, 2011.
- [2] N. Amarasingam, A. S. A. Salgadoe, K. Powell, L. F. Gonzalez, and S. Natarajan, "A review of uav platforms, sensors, and applications for monitoring of sugarcane crops," *Remote Sensing Applications: Society and Environment*, vol. 26, p. 100712, 2022.
- [3] Y. Zhao, W. Zheng, W. Xiao, S. Zhang, X. Lv, and J. Zhang, "Rapid monitoring of reclaimed farmland effects in coal mining subsidence area using a multi-spectral uav platform," *Environmental Monitoring and Assessment*, vol. 192, pp. 1–19, 2020.
- [4] A. Gholizadeh and V. Kopačková, "Detecting vegetation stress as a soil contamination proxy: A review of optical proximal and remote sensing techniques," *International Journal of Environmental Science and Technology*, vol. 16, pp. 2511–2524, 2019.
- [5] T. Shi, Y. Chen, Y. Liu, and G. Wu, "Visible and near-infrared reflectance spectroscopy—an alternative for monitoring soil contamination by heavy metals," *Journal of hazardous materials*, vol. 265, pp. 166–176, 2014.
- [6] B. Ma, A. Xu, X. Zhang, and L. Wu, "Chlorophyll change and spectral response of maize seedling under iron stress," in *2016 IEEE International Geoscience and Remote Sensing Symposium (IGARSS)*. IEEE, 2016, pp. 6397–6400.
- [7] A. Basile, S. Sorbo, G. Aprile, B. Conte, R. C. Cobianchi, T. Pisani, and S. Loppi, "Heavy metal deposition in the italian "triangle of death" determined with the moss *scorpiurum circinatum*," *Environmental Pollution*, vol. 157, no. 8-9, pp. 2255–2260, 2009.
- [8] C. Zhang, K. Yang, and W. Gao, "An experimental study on the influence of copper and lead concentration on the spectral reflectance of maize leaves," *Remote Sensing Letters*, vol. 11, no. 12, pp. 1147–1156, 2020.
- [9] R. Serrano-Calvo, M. E. Cutler, and A. G. Bengough, "Spectral and growth characteristics of willows and maize in soil contaminated with a layer of crude or refined oil," *Remote Sensing*, vol. 13, no. 17, p. 3376, 2021.

SHORT PAPER TITLE

- [10] C. Götze, A. Jung, I. Merbach, R. Wennrich, and C. Gläßer, “Spectrometric analyses in comparison to the physiological condition of heavy metal stressed floodplain vegetation in a standardised experiment,” *Open Geosciences*, vol. 2, no. 2, pp. 132–137, 2010.
- [11] L. A. Goldberger and A. C. Eden, “Multispectral and thermal imager onboard aerial platforms instrument handbook,” Oak Ridge National Lab.(ORNL), Oak Ridge, TN (United States). Atmospheric . . . , Tech. Rep., 2022.
- [12] M. T. Abdullayeva and G. T. Parpiyev, “The importance of using drones in monitoring agricultural crops,” *American Journal Of Agriculture And Horticulture Innovations*, vol. 2, no. 10, pp. 24–31, 2022.
- [13] S. Zhang, X. Xue, C. Chen, Z. Sun, and T. Sun, “Development of a low-cost quadrotor uav based on adrc for agricultural remote sensing,” *International Journal of Agricultural and Biological Engineering*, vol. 12, no. 4, pp. 82–87, 2019.
- [14] S. Gürtler, C. Souza Filho, I. Sanches, M. Alves, and W. Oliveira, “Determination of changes in leaf and canopy spectra of plants grown in soils contaminated with petroleum hydrocarbons,” *ISPRS Journal of Photogrammetry and Remote Sensing*, vol. 146, pp. 272–288, 2018.
- [15] M. Guizar-Sicairos, S. T. Thurman, and J. R. Fienup, “Efficient subpixel image registration algorithms,” *Optics letters*, vol. 33, no. 2, pp. 156–158, 2008.
- [16] Á. Maresma, M. Ariza, E. Martínez, J. Lloveras, and J. A. Martínez-Casasnovas, “Analysis of vegetation indices to determine nitrogen application and yield prediction in maize (zea mays l.) from a standard uav service,” *Remote Sensing*, vol. 8, no. 12, p. 973, 2016.
- [17] A. C. Kyrtziz, D. P. Skarlatos, G. C. Menexes, V. F. Vamvakousis, and A. Katsiotis, “Assessment of vegetation indices derived by uav imagery for durum wheat phenotyping under a water limited and heat stressed mediterranean environment,” *Frontiers in Plant Science*, vol. 8, p. 1114, 2017.
- [18] L. Qiao, W. Tang, D. Gao, R. Zhao, L. An, M. Li, H. Sun, and D. Song, “Uav-based chlorophyll content estimation by evaluating vegetation index responses under different crop coverages,” *Computers and Electronics in Agriculture*, vol. 196, p. 106775, 2022.
- [19] H. Q. Liu and A. Huete, “A feedback based modification of the ndvi to minimize canopy background and atmospheric noise,” *IEEE transactions on geoscience and remote sensing*, vol. 33, no. 2, pp. 457–465, 1995.
- [20] W. Gao, K. Yang, G. Chen, Y. Li, Q. Han, and B. Wu, “Discrimination of heavy metal crop contamination using measurements of leaf spectra,” *Remote Sensing Letters*, vol. 12, no. 3, pp. 278–285, 2021.
- [21] C. Boente, L. Salgado, E. Romero-Macías, A. Colina, C. A. López-Sánchez, and J. L. R. Gallego, “Correlation between geochemical and multispectral patterns in an area severely contaminated by former hg-as mining,” *ISPRS International Journal of Geo-Information*, vol. 9, no. 12, p. 739, 2020.
- [22] S. A. Anjum, U. Ashraf, I. Khan, M. Tanveer, M. F. Saleem, and L. Wang, “Aluminum and chromium toxicity in maize: implications for agronomic attributes, net photosynthesis, physio-biochemical oscillations, and metal accumulation in different plant parts,” *Water, Air, and Soil Pollution*, vol. 227, pp. 1–14, 2016.
- [23] M. WAHBA, L. Fawkia, and A. Zaghoul, “Management of calcareous soils in arid region,” *International Journal of Environmental Pollution and Environmental Modelling*, vol. 2, no. 5, pp. 248–258, 2019.
- [24] A. Lafuente, C. González, J. Quintana, A. Vázquez, and A. Romero, “Mobility of heavy metals in poorly developed carbonate soils in the mediterranean region,” *Geoderma*, vol. 145, no. 3-4, pp. 238–244, 2008.
- [25] B. J. Alloway, “Soil factors associated with zinc deficiency in crops and humans,” *Environmental geochemistry and health*, vol. 31, no. 5, pp. 537–548, 2009.
- [26] A. Suganya, A. Saravanan, and N. Manivannan, “Role of zinc nutrition for increasing zinc availability, uptake, yield, and quality of maize (zea mays l.) grains: An overview,” *Commun. Soil Sci. Plant Anal*, vol. 51, no. 15, pp. 2001–2021, 2020.
- [27] A. Piccolo, “The supramolecular structure of humic substances: a novel understanding of humus chemistry and implications in soil science,” 2002.

- [28] E. Puglisi, G. Fragoulis, A. A. Del Re, R. Spaccini, A. Piccolo, G. Gigliotti, D. Said-Pullicino, and M. Trevisan, "Carbon deposition in soil rhizosphere following amendments with compost and its soluble fractions, as evaluated by combined soil-plant rhizobox and reporter gene systems," *Chemosphere*, vol. 73, no. 8, pp. 1292–1299, 2008.
- [29] M. Piri, E. Sepehr, and Z. Rengel, "Citric acid decreased and humic acid increased zn sorption in soils," *Geoderma*, vol. 341, pp. 39–45, 2019.
- [30] S. Nardi, D. Pizzeghello, A. Muscolo, and A. Vianello, "Physiological effects of humic substances on higher plants," *Soil Biology and Biochemistry*, vol. 34, no. 11, pp. 1527–1536, 2002.
- [31] L. P. Canellas and F. L. Olivares, "Physiological responses to humic substances as plant growth promoter," *Chemical and Biological Technologies in Agriculture*, vol. 1, no. 1, pp. 1–11, 2014.